ELSEVIER

Journal of the Neurological Sciences 264 (2008) 73–76

Journal of the Neurological Sciences

www.elsevier.com/locate/jns

Novel *SACS* mutation in a Belgian family with sacsin-related ataxia

Y. Ouyang [a,e], K. Segers [b], O. Bouquiaux [c], F.C. Wang [d], N. Janin [b], C. Andris [f], H. Shimazaki [a], K. Sakoe [a], I. Nakano [a], Y. Takiyama [a,*]

[a] *Division of Neurology, Department of Internal Medicine, Jichi Medical University, Tochigi 329-0498, Japan*
[b] *Department of Human Genetics, Hôpital du Sart Tilman, Liege, Belgium*
[c] *Department of Neurology, Centre Hospitalier de l'Ardenne, Libramont, Belgium*
[d] *Department of Neurology, Hôpital du Sart Tilman, Liege, Belgium*
[e] *Department of Neurology, The First Affiliated Hospital, China Medical University, Shenyang 110001, Liaoning Province, China*
[f] *Department of Neurology, Hôpital du Sart Tilman, Liege, Belgium*

Received 21 May 2007; received in revised form 15 July 2007; accepted 20 July 2007
Available online 22 August 2007

Abstract

The authors describe the four patients in the first known Belgian family with autosomal recessive spastic ataxia of Charlevoix–Saguenay (ARSACS). A novel homozygous missense mutation, NM_014363.3: c.3491T>A in exon 9, of the *SACS* gene was identified in the present family, which results in an original amino acid of methionine to lysine substitution at amino acid residue 1164 (p.M1164K). Although the cardinal clinical features, i.e., spastic ataxia with peripheral neuropathy, in our patients were similar to those in Quebec patients, our patients exhibited some atypical clinical features, e.g., teenage-onset and absence of retinal hypermyelination. The present family is from Wallonia, and there could be shared ethnicity with the families of Charlevoix–Saguenay.

Keywords: ARSACS; The *SACS* gene; Belgian family; Teenage-onset

1. Introduction

Autosomal recessive spastic ataxia of Charlevoix–Saguenay (ARSACS; OMIM 270550) is an inherited neurodegenerative disorder characterized by early-onset spastic ataxia, dysarthria, nystagmus, distal muscle wasting, finger and/or foot deformities, and retinal hypermyelination. It was originally described, with a high prevalence among inhabitants of the Charlevoix–Saguenay region of north-eastern Quebec in Canada, in the late 1970s [1].

In 2000, the gene responsible for ARSACS (*SACS*) was mapped to 13q11. The *SACS* gene was initially reported to consist of a single gigantic exon spanning 12.8kb with an 11.5-kb open reading frame (ORF), which encodes the protein sacsin [2]. However, eight exons upstream from the gigantic one were very recently found, and thus the new ORF is 13,299 bp long. To date, approximately 30 mutations have been reported in Quebec and non-Quebec patients [3–5], and ARSACS is now global [6]. We report here a novel *SACS* mutation in a Belgian family with ARSACS.

2. Methods

We encountered four patients in a Belgian family with teenage-onset ataxia. This family is from Wallonia, and more exactly from 'les Ardennes'. There was distant consanguinity between the two pairs of parents (II-1 and II-2, and II-3 and II-4), but the detailed relationship was unknown (Fig. 1). Detailed neurological examination was performed on the whole family, i.e., the patients and unaffected individuals.

Blood samples were obtained with informed consent from 12 individuals in this family. Genomic DNA was extracted from peripheral blood leukocytes. Using 38 appropriate primer pairs (all primer sequences are available on request), the coding exons of the *SACS* gene were amplified by PCR from 200 ng of genomic DNA, and then sequenced directly with an ABI PRISM 3100 genetic analyzer; the analysis was

* Corresponding author. Tel.: +81 285 58 7352; fax: +81 285 44 5118.
E-mail address: ytakiya@jichi.ac.jp (Y. Takiyama).

0022-510X/$ - see front matter © 2007 Elsevier B.V. All rights reserved.
doi:10.1016/j.jns.2007.07.022

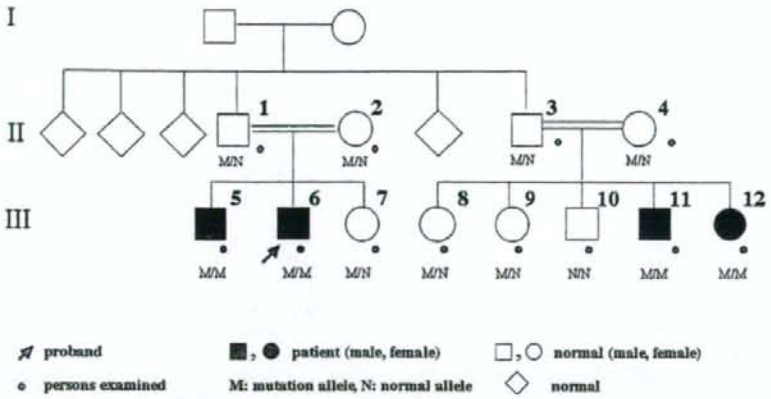

Fig. 1. Pedigree of the Belgian family with ARSACS. There was distant consanguinity between the two pairs of parents (II-1 and II-2, and II-3 and II-4), but the detailed relationship was unknown. The gender is concealed for some individuals, denoted by diamonds, to maintain the anonymity of the family.

performed with Sequencing Analysis software, ver. 5.2 (Applied Biosystems), as described previously [7–9]. When sequence analysis revealed a novel missense mutation in the Belgian family, we examined 114 Belgian control chromosomes in order to exclude polymorphisms. The PCR products containing the novel mutation with specific primers (1410F, 5′-TTGGCTCCTCACTTCCTCTTGTTG-3′; 1962R, 5′-ACTGGTGTGTTGGGGCTTGCT-3′) were digested with *Nco I* (Takara Bio Inc.) at 37 °C overnight, subjected to electrophoresis on 3.5% NuSieve 3:1 agarose gels, and then stained with ethidium bromide. The wild-type PCR products harbor three *Nco I* sites, one of which is destroyed by the novel missense mutation.

This study was approved by the Medical Ethical Committee of Jichi Medical University.

3. Results

3.1. Clinical study

We found four patients (III-5, III-6, III-11, and III-12) with progressive gait unsteadiness in a Belgian family. The age at onset was 13, 12, 12, and 13 years old, respectively, and the age at examination ranged from 21 to 43 years old. There were no obvious abnormalities in their first decade. All of the patients, however, complained that their gait and running became slow and unsteady at the start of their second decade. It became difficult for them to do sports or gymnastic exercise in their school days.

Neurological examination revealed that cerebellar ataxia with leg spasticity was a cardinal clinical feature in all four patients (Table 1). Furthermore, all patients showed absent ankle jerks and pes cavus. The Babinski sign was present in three patients, but equivocal in one patient with hyperreflexia. Distal amyotrophy was apparent in three patients. Myelinated retinal nerve fibers were not apparent in one patient examined ophthalmologically. Mini Mental State Examination was 30/30 in all patients. Brain MRI was performed in all patients, which revealed cerebellar atrophy, particularly in the vermis (data not shown). Motor nerve conduction velocity examination in one patient (III-6) revealed mild reduction in the median and ulnar nerves, and moderate reduction in the common peroneal nerves. A compound muscle action potential was not evoked in the posterior tibial nerve. A sensory nerve action potential was not evoked in the radial and sural nerves (data not shown). The other three patients showed similar data in the peripheral nerve conduction study.

3.2. Molecular study

A homozygous missense mutation, NM_014363.3: c.3491T>A in exon 9 of the *SACS* gene, was identified in our patients (Fig. 2), which results in an original amino acid of methionine to lysine substitution at amino acid residue 1164 (p.M1164K). This substitution was found to be heterozygous in the four unaffected parents (II-1, II-2, II-3,

Table 1
Summary of the neurological findings in the patients in the Belgian family

Patient	III-5	III-6	III-11	III-12
Age (years)	43	41	34	33
Sex	M	M	M	F
Age at onset (years)	13	12	12	13
Age at examination (years)	43	39	35	21
Cerebellar ataxia	+	+	+	+
Dysarthria	+	+	+	–
Nystagmus	+	+	+	+
Distal amyotrophy	+	+	+	–
Absent ankle jerks	+	+	+	+
Babinski sign	+	+	+	*
Hyperreflexia	+	–	+	+
Leg spasticity	+	+	+	+
Finger deformity	+	?	?	–
Pes cavus	+	+	+	+
Retinal myelinated fibers	NE	–	NE	NE
MMSE	30/30	30/30	30/30	30/30

M: Male, F: female, MMSE: Mini Mental State Examination, NE: not examined, *: equivocal.

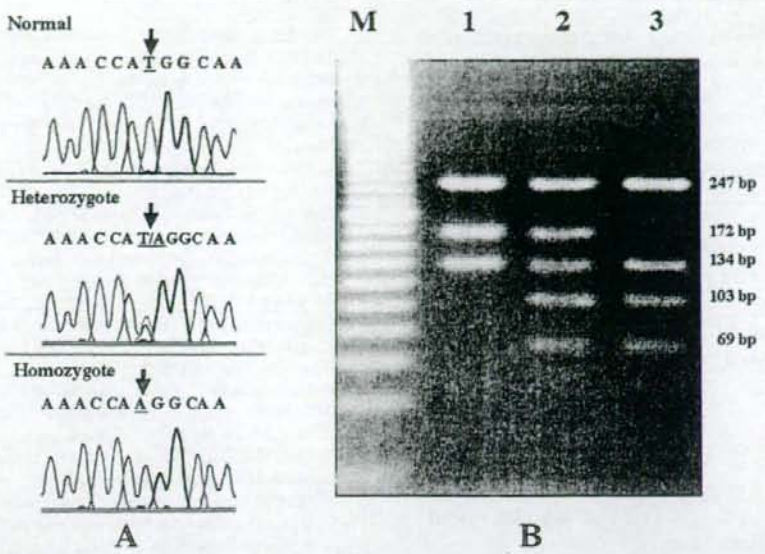

Fig. 2. A. Identification of a novel missense mutation of the *SACS* gene in the Belgian family. The sequences in a normal control, a carrier, and a patient are shown in the upper, middle, and lower panels, respectively. The arrow indicates the NM_014363.3: c.3491T>A substitution with a heterozygous or a homozygous state. B. The PCR products after *Nco I* digestion. Lane M, 20 bp size markers. Lane 1, the *Nco I*-digested PCR products with a homozygous NM_014363.3: c.3491T>A substitution (patient) gave three bands (247, 172, and 134 bp). Lane 2, the *Nco I*-digested PCR products with a heterozygous NM_014363.3: c.3491T>A substitution (carrier) gave five bands (247, 172, 134, 103, and 69 bp). Lane 3, the wild-type *Nco I*-digested PCR products gave four bands (247, 134, 103, and 69 bp).

and II-4) and three siblings (III-7, III-8, and III-9), but not in the other unaffected one, III-10 (Fig. 1). Thus, this novel missense mutation in exon 9 of the *SACS* gene was found to be cosegregated with the disease in the Belgian family with autosomal recessive transmission. Furthermore, this mutation was not found in 114 Belgian control chromosomes.

4. Discussion

Although mutations of the *SACS* gene were originally identified in Quebec patients [2], *SACS* mutations have been reported in non-Quebec patients including ones in Japan, Italy, Tunisia, Turkey, and Spain so far [3–5,7–13]. In this study, we examined the first Belgian family with a *SACS* mutation. The present family is from Wallonia, and there could be shared ethnicity with families of Charlevoix–Saguenay.

Genetically, the present missense mutation (NM_014363.3: c.3491T>A) is considered to be responsible for our patients' disease, because this novel mutation was cosegregated with the disease in the Belgian family with autosomal recessive transmission. Furthermore, the mutation was not found in 114 Belgian control chromosomes. In addition, p.M1164K leads to a change in the secondary structure predicted by the PROF program [14]. To date, although the genotype is expanding upstream from the original gigantic exon 9 [5,7], more than 90% of the causative *SACS* mutations, including ours, have been detected in exon 9 [3,4]. Furthermore, two important domains, i.e., the DnaJ molecular chaperone homology domain and the HEPN (Higher Eukaryotes and Prokaryotes Nucleotide-binding) domain, correlate with chaperone-mediated protein folding in the *SACS* protein, and are encoded by exon 9. Thus, exon 9 may play an important role in the function of sacsin, and it should be preferentially analyzed when performing a molecular test on ARSACS.

The cardinal clinical features and MRI findings in our patients are similar to those in Quebec ones with ARSACS reported previously, such as a progressive ataxic gait, dysarthria, nystagmus, leg spasticity, the Babinski sign, hyperreflexia, foot deformity, pes cavus, normal intelligence, peripheral neuropathy, and atrophy of the cerebellar vermis [1–4]. In addition, the neurophysiological data closely resemble those previously reported [3,4,8,9], suggesting that severe axonal degeneration and diffuse peripheral demyelination are general in ARSACS.

One patient, however, showed the absence of retinal hypermyelination. Although this feature is atypical in Quebec patients [1], it has sometimes been reported in non-Quebec ones [4,5]. Thus, the present study confirmed that retinal hypermyelination is variable in non-Quebec patients.

Furthermore, all our patients showed teenage-onset ataxia (12–13 years old). Since the age of onset in ARSACS usually ranges from infancy to preschool age (from 2 to 5.5 years old) [4], that in our patients was much later than that in Quebec and most non-Quebec patients, except for in two non-Quebec families (age of onset, 10 and 12 years old)

[5,11]. The identification of teenage-onset cases of different races suggests that the onset age in ARSACS might vary.

Meanwhile, since the clinical features of teenage-onset ARSACS are similar to those of autosomal recessive spastic ataxia such as SPG30 (mean onset age, 17.5 years) [15] and SAX2 (onset age, before 15 years) [16], it is necessary to discriminate these diseases in patients with teenage-onset spastic ataxia.

In conclusion, this is the first documentation of a Belgian ARSACS family. Since the present family is from Wallonia, identification of a novel mutation of the *SACS* gene would be of interest. As more *SACS* mutations are identified, the clinical spectrum of sacsinopathies might expand.

Acknowledgements

The authors thank the family for participating in this study. This work was supported by a grant from the Research Committee for Ataxic Diseases (Y.T.) of the Ministry of Health, Labor and Welfare, Japan.

References

[1] Bouchard JP, Barbeau A, Bouchard R, Bouchard RW. Autosomal recessive spastic ataxia of Charlevoix–Saguenay. Can J Neurol Sci 1978;5:61–9.
[2] Engert JC, Bérubé P, Mercier J, Dore C, Lepage P, Ge B, et al. ARSACS, a spastic ataxia common in northeastern Québec, is caused by mutations in a new gene encoding an 11.5-kb ORF. Nat Genet 2000;24:120–5.
[3] Takiyama Y. Autosomal recessive spastic ataxia of Charlevoix–Saguenay. Neuropathology 2006;26:368–75.
[4] Takiyama Y. Sacsinopathies: sacsin-related ataxia. Cerebellum 2007:6.
[5] Takado Y, Hara K, Shimohata T, Tokiguchi S, Onodera O, Nishizawa M. New mutation in the non-gigantic exon of SACS in Japanese siblings. Mov Disord 2007;22:748–9.
[6] Gomez CM. A.R.S.A.C.S., goes global. Neurology 2004;62:10–1.
[7] Ouyang Y, Takiyama Y, Sakoe K, Shimazaki H, Ogawa T, Nagano S, et al. Sacsin-related ataxia (ARSACS): expanding the genotype upstream from the gigantic exon. Neurology 2006;66:1103–4.
[8] Shimazaki H, Takiyama Y, Sakoe K, Ando Y, Nakano I. A phenotype without spasticity in sacsin-related ataxia. Neurology 2005;64:2129–31.
[9] Shimazaki H, Sakoe K, Niijima K, Nakano I, Takiyama Y. An unusual case of a spasticity-lacking phenotype with a novel SACS mutation. J Neurol Sci 2007;255:87–9.
[10] Criscuolo C, Banfi S, Orio M, Gasparini P, Monticelli A, Scarano V, et al. A novel mutation in SACS gene in a family from southern Italy. Neurology 2004;62:100–2.
[11] El Euch-Fayache G, Lalani I, Amouri R, Turki I, Ouahchi K, Hung WY. Phenotypic features and genetic findings in sacsin-related autosomal recessive ataxia in Tunisia. Arch Neurol 2003;60:928–82.
[12] Richter AM, Ozgul RK, Poisson VC, Topaloglu H. Private SACS mutations in autosomal recessive spastic ataxia of Charlevoix–Saguenay (ARSACS) families from Turkey. Neurogenetics 2004;5:165–70.
[13] Criscuolo C, Sacca F, De Michele G, Mancini P, Combarros O, Infante J, et al. Novel mutation of SACS gene in a Spanish family with autosomal recessive spastic ataxia. Mov Disord 2005;20:1358–61.
[14] Rost B, Sander C. Prediction of protein secondary structure at better than 70% accuracy. J Mol Biol 1993;232:584–99.
[15] Krebe S, Azzedine H, Durr A, Bastien P, Bouslam N, Elleuch N, et al. Autosomal recessive spastic paraplegia (SPG30) with mild ataxia and sensory neuropathy maps to chromosome 2q37.3. Brain 2006;129:1456–62.
[16] Bouslam N, Bouhouche A, Benomar A, Hanein S, Klebe S, Azzedine H, et al. A novel locus for autosomal recessive spastic ataxia on chromosome 17p. Hum Genet 2007;121:413–20 [Published online].

Phosphorylated TDP-43 in Frontotemporal Lobar Degeneration and Amyotrophic Lateral Sclerosis

Masato Hasegawa, PhD,[1] Tetsuaki Arai, MD, PhD,[2] Takashi Nonaka, PhD,[1] Fuyuki Kametani, PhD,[1] Mari Yoshida, MD, PhD,[3] Yoshio Hashizume, MD, PhD,[3] Thomas G. Beach, MD, PhD,[4] Emanuele Buratti, PhD,[5] Francisco Baralle, MD, PhD,[5] Mitsuya Morita, MD, PhD,[6] Imaharu Nakano, MD, PhD,[6] Tatsuro Oda, MD, PhD,[7] Kuniaki Tsuchiya, MD, PhD,[8] and Haruhiko Akiyama, MD, PhD[2]

Objective: TAR DNA-binding protein of 43kDa (TDP-43) is deposited as cytoplasmic and intranuclear inclusions in brains of patients with frontotemporal lobar degeneration with ubiquitinated inclusions (FTLD-U) and amyotrophic lateral sclerosis (ALS). Previous studies reported that abnormal phosphorylation takes place in deposited TDP-43. The aim of this study was to identify the phosphorylation sites and responsible kinases, and to clarify the pathological significance of phosphorylation of TDP-43.

Methods: We generated multiple antibodies specific to phosphorylated TDP-43 by immunizing phosphopeptides of TDP-43, and analyzed FTLD-U and ALS brains by immunohistochemistry, immunoelectron microscopy, and immunoblots. In addition, we performed investigations aimed at identifying the responsible kinases, and we assessed the effects of phosphorylation on TDP-43 oligomerization and fibrillization.

Results: We identified multiple phosphorylation sites in carboxyl-terminal regions of deposited TDP-43. Phosphorylation-specific antibodies stained more inclusions than antibodies to ubiquitin and, unlike existing commercially available anti–TDP-43 antibodies, did not stain normal nuclei. Ultrastructurally, these antibodies labeled abnormal fibers of 15nm diameter and on immunoblots recognized hyperphosphorylated TDP-43 at 45kDa, with additional 18 to 26kDa fragments in sarkosyl-insoluble fractions from FTLD-U and ALS brains. The phosphorylated epitopes were generated by casein kinase-1 and -2, and phosphorylation led to increased oligomerization and fibrillization of TDP-43.

Interpretation: These results suggest that phosphorylated TDP-43 is a major component of the inclusions, and that abnormal phosphorylation of TDP-43 is a critical step in the pathogenesis of FTLD-U and ALS. Phosphorylation-specific antibodies will be powerful tools for the investigation of these disorders.

Ann Neurol 2008;64:60–70

Tau-negative and ubiquitin-positive inclusions (UPIs) that include neuronal cytoplasmic inclusions (NCIs), neuronal intranuclear inclusions (NIIs), and dystrophic neurites (DNs) are the pathological hallmarks of frontotemporal lobar degeneration with ubiquitinated inclusions (FTLD-U) with or without clinical features of motor neuron disease (MND).[1] Recently, several genes and chromosomal loci, including the progranulin *(PGRN)* gene,[2,3] valosin-containing protein *(VCP)* gene,[4] and an unidentified site at chromosome 9p,[5,6] have been reported to be associated with familial FTLD-U. Ubiquitin-positive, tau-negative NCIs have also been recognized in patients with the classic type of MND, amyotrophic lateral sclerosis (ALS),[7] in which skein-like cytoplasmic inclusions are found in the lower motor neurons of the hypoglossal nucleus and spinal cord.[8,9] In both FTLD-U and ALS, understanding why these inclusions form may provide critical clues to the neurodegenerative process.

Recently, TAR DNA-binding protein of 43kDa

From the Departments of [1]Molecular Neurobiology and [2]Psychogeriatrics, Tokyo Institute of Psychiatry, Tokyo Metropolitan Organization for Medical Research, Kamikitazawa, Setagaya-ku, Tokyo; [3]Department of Neuropathology, Institute for Medical Science of Aging, Aichi Medical University, Yazako, Nagakute-cho, Aichi-gun, Aichi, Japan; [4]Sun Health Research Institute, Sun City, AZ; [5]International Centre for Genetic Engineering and Biotechnology, Trieste, Italy; [6]Department of Neurology, Jichi Medical University, Shimotsuke-shi, Tochigi; [7]Department of Neuropsychiatry, National Shimofusa Mental Hospital, Chiba; and [8]Department of Laboratory Medicine and Pathology, Tokyo Metropolitan Matsuzawa Hospital, Setagaya-ku, Tokyo, Japan.

Received Nov 8, 2007, and in revised form April 8, 2008. Accepted for publication April 22, 2008.

Published online in Wiley InterScience (www.interscience.wiley.com). DOI: 10.1002/ana.21425

Address correspondence to Drs Hasegawa and Arai, Departments of Molecular Neurobiology and Psychogeriatrics, Tokyo Institute of Psychiatry, Tokyo Metropolitan Organization for Medical Research, 2-1-8 Kamikitazawa, Setagaya-ku, Tokyo 156-8585. E-mail: masato@prit.go.jp

(TDP-43), which functions in regulating transcription and alternative splicing,[10,11] was identified as a component of these UPIs.[12–14] TDP-43 appears to belong to the group of two RNA-binding domain-Gly RNA-binding proteins, which include the heterogeneous nuclear ribonucleoprotein (hnRNP) family and factors involved in RNA splicing and transport.[15] TDP-43 binds hnRNP A/B and hnRNP A1 through its C-terminal region, inhibiting premessenger RNA splicing.[16] Several disorders, including FTLD-U, FTLD-MND, and ALS are now referred to as TDP-43 proteinopathies.[12–14] Immunoblot analysis of the sarkosyl-insoluble fraction extracted from brains of patients afflicted with these disorders shows an abnormal TDP-43–immunoreactive band at 45kDa. The electric mobility of this band changes after dephosphorylation, suggesting that abnormal phosphorylation takes place in accumulated TDP-43.[12,13] However, the phosphorylation sites, responsible kinases, and pathological significance of phosphorylation are still unknown.

In this report, we demonstrate that multiple antibodies raised against TDP-43 phosphopeptides label UPIs in histological sections from FTLD-U and ALS brains. These antibodies may offer advantages over previous antibodies used to identify these structures because they appear to be more sensitive than anti-ubiquitin antibodies and, unlike commercially available anti–TDP-43 antibodies, do not stain normal neuronal nuclei. In addition, these antibodies specifically recognize abnormal TDP-43 species on immunoblots of sarkosyl-insoluble fractions extracted from FTLD-U and ALS brains. Furthermore, we show that the multiple phosphorylation epitopes identified in aggregated TDP-43 are generated by casein kinase-1 (CK1), and that oligomerization or fibril formation of TDP-43 is promoted by phosphorylation with CK1 in vitro. These results suggest that phosphorylated TDP-43 is a critical component of UPIs in FTLD-U and ALS, and that phosphorylation of TDP-43 by CK1 may be involved in the accumulation of the protein.

Subjects and Methods

Materials

Human brain tissue was obtained from the Brain Donation Program at Sun Health Research Institute (Sun City, AZ), Aichi Medical University (Japan), Jichi Medical University (Japan), National Shimofusa Mental Hospital (Japan), and Tokyo Metropolitan Matsuzawa Hospital (Japan). Small blocks of brain tissue were dissected at autopsy and frozen rapidly at −70 to 80°C or fixed in 4% paraformaldehyde in 0.1M phosphate buffer (pH 7.4) for 2 days. Brain tissue from sporadic FTLD-U, familial FTLD-U with PGRN mutations (mPGRN), sporadic ALS, and sporadic FTLD-MND was compared with brain tissue from Alzheimer's disease (AD) and neurologically normal control subjects. The age, sex, brain regions examined, diagnosis, and histopathological subtyping for these cases are given in Table 1. Neuropathological diagnoses of FTLD-U, FTLD-MND, ALS, and AD were made in accordance with published guidelines.[1,9,17–19]

Table 1. **Subjects, Brain Regions, Pathological Diagnosis, and Subtypes Examined**

Case No.	Age (yr)	Sex	Region	Diagnosis	Subtype
1	67	M	Hip, T, F	FTLD-U (sporadic)	1
2	59	M	Hip, T	FTLD-U (sporadic)	1
3	68	F	Hip, T	FTLD-U (sporadic)	1
4	49	F	T	FTLD-MND	2
5	76	M	Prec	FTLD-MND	2
6	66	M	F, SC	ALS	2
7	70	M	Prec, SC	ALS	2
8	69	M	Prec	ALS	2
9	53	M	Hip, T, F	FTLD-U (mRGRN)	3
10	56	F	Hip, T, F	FTLD-U (mRGRN)	3
11	54	M	Hip, T, F	FTLD-U (mRGRN)	3
12	68	F	Hip, T	AD	—
13	83	F	Hip, T	AD	—
14	65	M	Hip, T	Control	—
15	72	M	Hip, T	Control	—

Hip = hippocampus; T = temporal; F = frontal; FTLD-U = frontotemporal lobar degeneration with ubiquitinated inclusions; MND = motor neuron disease; Prec = precentral; SC = spinal cord; ALS = amyotrophic lateral sclerosis; mPGRN = mutations of progranulin gene; AD = Alzheimer's disease.

Although none of the three ALS cases had a documented history of dementia, all had immunohistochemical evidence of pathology in the neocortex.

Preparation of Antibodies

Immunogens consisted of 39 synthetic phosphopeptides representing 36 of the 64 Ser/Thr/Tyr sites in the human TDP-43 molecule. All peptides were conjugated at the amino or carboxyl terminal by a cysteine linkage to synthetic thyroglobulin using m-maleimidobenzoyl-*N*-hydroxysuccinimide ester as a coupling reagent.[20] The rabbit antisera were purified by obtaining flow-through fractions from a Toyopearl AF-Tresyl-650M (TOSOH, Tokyo, Japan) or SulfoLink Coupling Gel (Pierce Biotechnology, Rockford, IL) precoated with the nonphosphorylated synthetic peptide. The specificities of the antibodies were verified by enzyme-linked immunosorbent assay and immunoblot. A phosphorylation-independent rabbit polyclonal antibody to TDP-43 was also produced using a C-terminal peptide of TDP-43 (405-414) as immunogen.

Immunohistochemistry

After cryoprotection in 15% sucrose in 0.01M phosphate-buffered saline (pH 7.4), paraformaldehyde-fixed tissue blocks were cut on a freezing microtome at 30μm thickness. The free-floating sections were immunostained with an anti-ubiquitin antibody (DF2, a gift from Dr Mori, 1:200),[21] a commercially obtained phosphorylation-independent anti-TDP-43 antibody (10782-1-AP; ProteinTech Group, Chicago, IL; 1:2,000), and a panel of phosphorylation-dependent anti-TDP-43 antibodies including pS409/410, using methods previously described.[13] Double-labeled immunofluorescence was performed using fluorescein isothiocianate- and tetramethylrhodamine isothiocyanate–conjugated secondary antibodies; sections were examined with a confocal laser microscope (LSM5 PASCAL; Carl Zeiss MicroImaging GmbH, Jena, Germany).

Immunoelectron Microscopy

Tissue blocks of ALS lumber spinal cord were fixed in paraformaldehyde and embedded in LR White Resin (London Resin, Reading, United Kingdom). Ultrathin sections were incubated with pS409/410 (1:1,000), and the immunoreaction products were probed using colloidal gold particles (1:10 dilution; BBinternational, Cardiff, United Kingdom) according to a standard immunogold-based postembedding electron microscopic procedure.[22]

Immunoblotting

Sarkosyl-insoluble, urea-soluble fractions were extracted from the frontal and the temporal regions of control, FTLD-U, and ALS brains as previously described.[23] The samples before (−) and after (+) the treatment with lambda protein phosphatase (λPPase) were loaded on 10% sodium dodecyl sulfate polyacrylamide gel electrophoresis. Proteins in the gel were then electrotransferred onto a polyvinylidene difluoride membrane (Millipore, Bedford, MA). After blocking with 3% gelatin in tris(hydroxymethyl)aminomethane (Tris)–buffered saline (50mM Tris-HCl, pH 7.5, 150mM NaCl), membranes were incubated overnight with the primary antibodies. After incubation with an appropriate biotinylated secondary antibody, labeling was detected as described previously.[13,23]

In Vitro Phosphorylation and Fibrillization of TDP-43

Human TDP-43 complementary DNA were subcloned into pRK172 expression vectors and transformed into *Escherichia coli* BL21(DE3). For in vitro phosphorylation, crude extracts from *E. coli* that expressed human TDP-43 were used to prepare partially purified TDP-43 using heparin-Toyopearl column chromatography and elution with 0.5M NaCl. The elutes were phosphorylated with CK1 (10,000U/ml; New England Biolabs, Beverly, MA), casein kinase-2 (CK2) (10,000U/ml; New England Biolabs), or glycogen synthase kinase-3β (GSK3β) (10,000U/ml; New England Biolabs) at 30°C for 14 hours. To study fibrillization, we incubated partially purified TDP-43 aliquots in 30mM Tris-HCl at pH 7.5 containing 4mM magnesium chloride, 2mM ATP, with or without CK1 (10,000U/ml) at 30°C for 3 days. A few drops of reaction solution was then applied to a carbon-coated copper grid and allowed to air-dry. The grid was placed on a drop of blocking solution (10mg/ml bovine serum albumin in phosphate-buffered saline) for 10 minutes and then placed on a drop of primary antibody (pS409/410, 1:200) for 2 hours at room temperature. After washing with 10mg/ml bovine serum albumin in phosphate-buffered saline, the grid was placed on a drop of the secondary antibody conjugated to 10nm colloidal gold particles (1:50; Sigma, St. Louis, MO) for 1 hour at room temperature. Finally, after another round of washing, the grid was negatively stained with 2% sodium phosphotungstate and examined with the electron microscopy (JEM-1230; JEOL, Akishime, Japan).

Results

Multiple Sites within TDP-43 Are Abnormally Phosphorylated in Frontotemporal Lobar Degeneration with Ubiquitinated Inclusions and Amyotrophic Lateral Sclerosis

There are multiple potential phosphorylation sites within human TDP-43, including 41 serine (Ser), 15 threonine (Thr), and 8 tyrosine (Tyr) residues. To identify the critical phosphorylation sites of TDP-43, we raised antibodies against 39 different synthetic phosphopeptides, representing 36 of 64 candidate phosphorylation sites (Table 2). The major strategy was to choose Ser and Thr residues that cover known protein kinase consensus phosphorylation motifs, including R-X-pSer/Thr for protein kinase A, pSer/Thr-X-X-Ser/Thr for CK1, pSer/Thr-X-X-E/D for CK2, and pSer/Thr-X-X-X-Ser for GSK3 and CK1. In addition, Ser/Thr residues in C-terminal region of TDP-43 were chosen because they are analogous to abnormal phosphorylation sites found in tau or α-synuclein.

Of the generated antibodies, pS379, pS403/404, pS409, pS410, and pS409/410 intensely immunostained the UPIs in FTLD-U and ALS, and demonstrated, on immunoblots of sarkosyl-insoluble fractions

Table 2. **Antigen Peptides for Immunization of Rabbits**

	Site	Antigen Peptide
1	pT8	EYIRVT(p)EDENDEC
2	pS20	PIEIPS(p)EDDGTC
3	pS29	GTVLLS(p)TVTAC
4	pT88	CNYPKDNKRKMDET(p)D
5	pS91	CDETDAS(p)SAVKVKR
6	pS92	CDETDASS(p)AVKVKR
7	pS91/92	DETDAS(p)S(p)AVKVC
8	pT103	CKRAVQKT(p)SDLIVLG
9	pS104	CKRAVQKTS(p)DLIVLG
10	pT116	PWKTT(p)EQDLKEC
11	pT141	KKDLKT(p)GHSKGC
12	pT153	CGFVRFT(p)EYETQVK
13	pS180	CKLPNS(p)KQSQDE
14	pS183	CPNSKQS(p)QDEPLR
15	pS190	CKQSQDEPLRS(p)RK
16	pT199	CT(p)EDMTEDLE
17	pT203	RCTEDMT(p)EDELR
18	pT233	CRAFADVT(p)FADDQ
19	pS254	IIKGIS(p)VKISC
20	pS258	CISVHIS(p)NAEPK
21	pS266	CPKHNS(p)NRQLER
22	pS273	CRQLERS(p)GRFGGN
23	pS292	CGFGNS(p)RGGGA
24	pS305	CNNQGS(p)NMGGG
25	pS317	CFGAFS(p)INPAM
26	pS332	CAALQS(p)SWGMM
27	pS350	CQSGPS(p)GNNQN
28	pS375	GNNSYS(p)GSNSGC
29	pS379	CSGSNS(p)GAAIG
30	pS389	CGWGSAS(p)NAGS
31	pS393	CASNAGS(p)GSGF
32	pS395	CAGSGS(p)GFNGG
33	pS403	CGFNGGFGS(p)SMD
34	pS404	CNGGFGSS(p)MDSK
35	pS403/404	CNGGFGS(p)S(p)MDSK
36	pS407	CGSSMDS(p)KSSGW
37	pS409	CMDSKS(p)SGWGM
38	pS410	CMDSKSS(p)GWGM
39	pS409/410	CMDSKS(p)S(p)GWGM

extracted from brains of the FTLD-U and ALS cases, an abnormal band of 45kDa but not the 43kDa band corresponding to normal TDP-43. The results suggest that these sites are phosphorylated in the abnormal aggregates of TDP-43 present in FTLD-U and ALS.

Immunohistochemical Characterization of Phosphorylated TDP-43

Immunohistochemical staining showed that five of the phosphorylation-specific anti-TDP-43 antibodies identified UPIs in both FTLD-U and ALS brains. Of the phosphorylation-specific antibodies, the immunoreactivity of pS409/410 was particularly robust (Fig 1). In comparison, the commercially obtained, phosphorylation-independent, anti–TDP-43 antibody labeled NCIs, DNs, and neuronal nuclei in the dentate gyrus (see Fig 1A) and the temporal cortex (see Fig 1B) of the sporadic FTLD-U cases, and skein-like inclusions and neuronal nuclei in the spinal cord of ALS cases (see Fig 1C). It was particularly difficult to distinguish the staining of NCIs from that of neuronal nuclei in the dentate gyrus of the sporadic FTLD-U cases (see Fig 1A). By contrast, NCIs and DNs were unambiguously identified by the phosphorylation-specific antibody pS409/410, with no nuclear staining (see Figs 1D, E). Similarly, pS409/410 clearly labeled skein-like (see Fig 1F) and glial inclusions (see Fig 1G) in the spinal cord, and NCIs in the frontal and precentral cortices of the FTLD-MND and ALS cases (see Fig 1H). Glial inclusions in the frontal and precentral regions of the FTLD-MND and ALS cases were also immunopositive (data not shown). In the cases of familial FTLD-U with PGRN mutations, pS409/410 intensely stained NCIs, DNs, and NIIs in the cerebral cortex (see Figs 1I–K) and abundant positive structures in the cerebral white matter (see Fig 1L). The results of double-immunofluorescence staining showed that pS409/410 identified more NCIs than the ubiquitin antibody (see Figs 1M–O).

Based on morphological aspects, TDP-43 proteinopathies have been classified into four subtypes.[24] Type 1 is characterized by DNs with few NCIs and no NIIs, type 2 has numerous NCIs with few DNs and no NIIs, type 3 has numerous NCIs and DNs and an occasional NII, and type 4 has numerous NIIs and DNs with few NCIs. Type 4 is specific for familial FTLD-U with mutations of valosin-containing protein *(VCP)* gene. In this study, using the commercial anti–TDP-43 antibody, all of the sporadic FTLD-U cases showed type 1 pathology, all FTLD-MND and ALS cases showed type 2 pathology, and all FTLD-U with mPGRN showed type 3 pathology, in agreement with previous reports.[24,25]

The staining patterns obtained with our phosphorylation-dependent antibodies were similar to those seen

with the commercial phosphorylation-independent antibody, suggesting that all of the inclusion types previously described contain phosphorylated TDP-43. Similar staining patterns were obtained using pS379 (Figs 2A–C), pS403/404 (see Figs 2D–F), pS409 (see Figs 2G–I), and pS410 (see Figs 2J–L). Preabsorption of the antibodies with phosphopeptide immunogens abolished the labeling of these structures (data not shown).

Immunoelectron microscopic examination of the

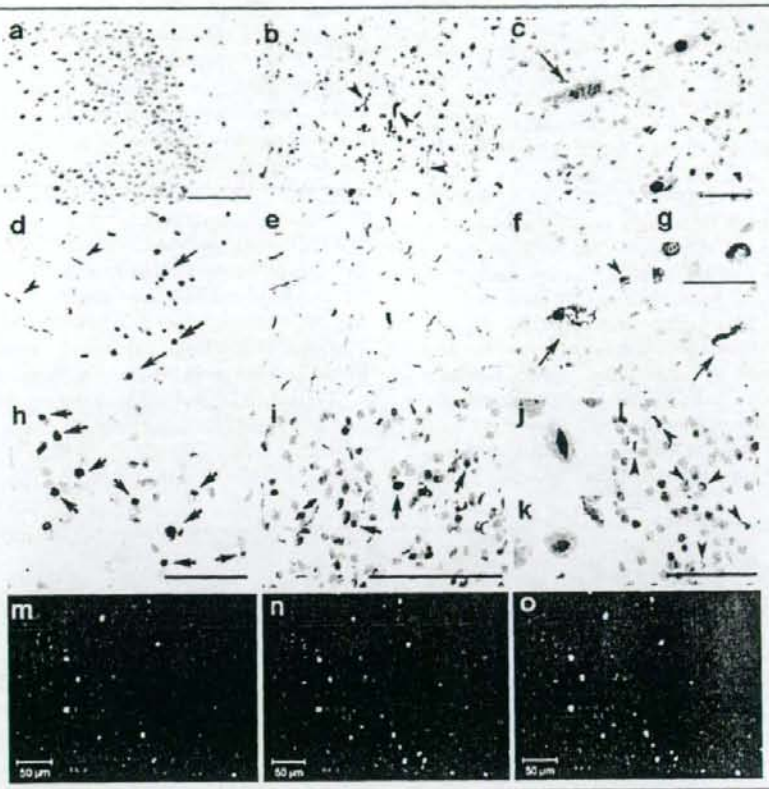

Fig 1. Immunohistochemical comparison of frontotemporal lobar degeneration with ubiquitinated inclusions (FTLD-U) and amyotrophic lateral sclerosis (ALS) brains using the phosphorylation-independent anti–TAR DNA-binding protein of 43kDa (TDP-43) antibody (ProteinTech) (A–C) and the phosphorylation-dependent anti–TDP-43 antibody (pS409/410) (D–L), in the dentate gyrus (A, D) and temporal cortex (B, E) of the sporadic FTLD-U cases, in the lumbar spinal cord (C, F, G) and the frontal cortex (H) of the ALS cases, and in the frontal cortex (I–K) and the frontal white matter (L) of the familial FTLD-U cases with progranulin (PGRN) mutations. (A) Because most of the nuclei of dentate gyrus granular neurons are immunopositive with the phosphorylation-independent antibody, it is difficult to identify neuronal cytoplasmic inclusions (NCIs). (B) TDP-43–positive dystrophic neurites (DNs) are recognizable (arrowheads) *in addition to the nuclei. (C) The* black arrow *indicates a cell with skein-like inclusions.* White arrows *and* arrowheads *indicate the normal nuclei of anterior horn cells and glial nuclei, respectively. Photomicrographs (D–F) illustrate the corresponding areas to (A–C), respectively. Note the absence of nuclear staining in (D–G) with the phosphorylation-dependent antibody pS409/410. (D) NCIs* (arrows) *and DNs* (arrowheads) *are clearly seen. (E) More abundant DNs are seen than in (B). (F)* Arrows *indicate skein-like inclusions;* arrowheads *indicate glial inclusions. (G, insert) Glial inclusions at a higher magnification. (H) NCIs in the frontal cortices of the ALS case are immunopositive. In the cases with PGRN mutations, pS409/410 clearly stains NCIs* (arrows), *DNs (I), and neuronal intranuclear inclusions (NIIs) (J, K) in the superficial cortical layers, and abundant immunopositive structures in the white matter (L,* arrowheads), *with no nuclear staining. Sections are counterstained with hematoxylin to show nuclei in (C, F–L). (M–O) Antiubiquitin (DF2) and pS409/410 double-label immunofluorescence histochemistry of the dentate gyrus in the FTLD-U case. Only some of the pS409/410-positive NCIs are also ubiquitin positive. (M) DF2; (N) pS409/410; (G) merge. Cell nuclei are stained with TO-PRO-3 (Invitrogen, Tokyo, Japan), producing a blue color. Scale bars = 100μm (A, B, D, E, I); 50μm (C, F, H, L); 25μm (G); 10μm (J, K).*

spinal cord motoneuron inclusions of an ALS patient with the pS409/410 antibody showed immunopositive abnormal fibers of 15nm in diameter (Figs 3A, B).

Immunoblot Analysis of Phosphorylated TDP-43

Immunoblot analyses of sarkosyl-insoluble fractions extracted from the brains of control, AD, FTLD-U, and ALS cases with the phosphorylation-independent TDP-43 antibody (ProteinTech) always showed a band of 43kDa and also showed an additional 45kDa band that was present only in FTLD-U and ALS cases, as described previously[12,13] (Fig 4A). The phosphorylation-dependent antibodies specific for pS409/410 (see Fig 4B), pS409 (see Fig 4C), pS410 (see Fig 4D), pS403/404 (see Fig 4E), and pS379 (see Fig 4F) did not recognize the normal 43kDa band, showing a single band at approximately 45kDa, several smaller fragments at approximately 25kDa, and indistinct smears in FTLD-U and ALS cases but not in control and AD cases (see Figs 4B–F). The intensity of the approximately 25kDa fragments tended to be greater than that of the 45kDa band in FTLD-U (see Figs 4B–E) and in ALS (see Figs 4B, D). As for the immunohistochemical findings, the antibody to pS409/410 showed the most intense labeling (see Fig 4B). All of the immunoreactive bands were completely abolished by dephosphorylation, which was performed with lambda protein phosphatase (8,000U/ml; New England Biolabs) at 30°C for 2 hours.

Immunoblot Distinction between Clinicopathological Subtypes of TDP-43

To investigate the biochemical basis of the different TDP-43 clinicopathological subtypes, we have carefully compared the results of immunoblots of the sarkosyl-insoluble, urea-soluble fractions from cerebral cortex of sporadic FTLD-U, FTLD-MND, ALS, and mPGRN cases. The results showed that the band patterns of the 18 to 26kDa fragments differed between clinicopathological subtypes (Figs 5A, B). Sporadic FTLD-U cases showed 2 major bands at 23 and 24kDa, and 2 minor bands at 18 and 19kDa, whereas FTLD-MND and ALS cases showed 3 major bands at 23, 24, and 26kDa, and 2 minor bands at 18 and 19kDa. A 23kDa band is the most intense in sporadic FTLD-U, whereas a 24kDa band is the most intense in FTLD-MND and ALS. Furthermore, the band pattern of mPGRN cases was not distinctive but intermediate between FTLD-U, FTLD-MND, and ALS cases.

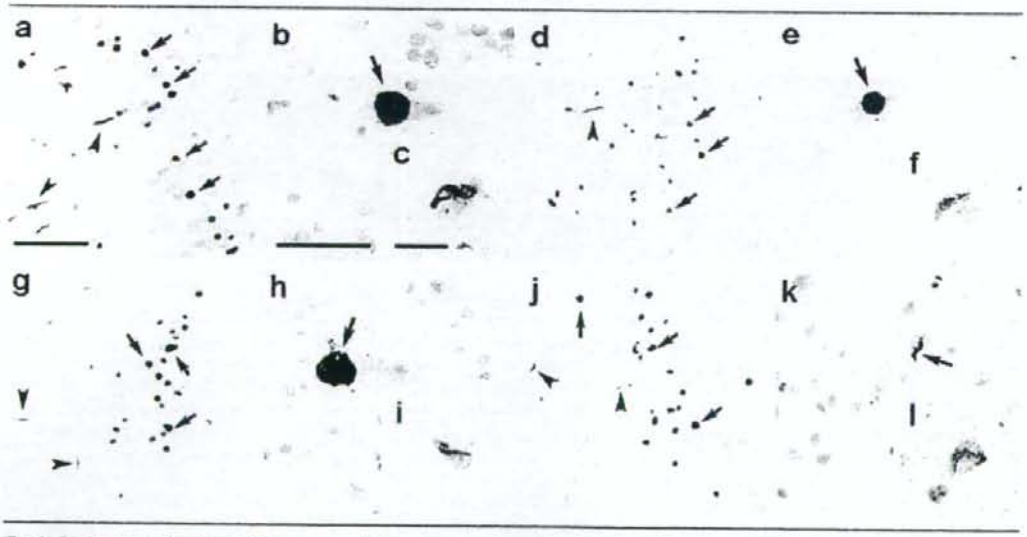

Fig 2. Immunohistochemistry of frontotemporal lobar degeneration with ubiquitinated inclusions (FTLD-U) brains and amyotrophic lateral sclerosis (ALS) spinal cords using the phosphorylation-dependent anti–TAR DNA-binding protein of 43kDa (TDP-43) antibodies specific for pS379 (A–C), pS403/404 (D–F), pS409 (G–I), and pS410 (J–L). These antibodies recognize neuronal cytoplasmic inclusions (NCIs) (arrows *in A, D, G, J) and dystrophic neurites (DNs)* (arrowheads *in A, D, G, J) in the dentate gyrus of the sporadic FTLD-U cases and motoneuronal round inclusions* (arrow *in B, E, H), skein-like inclusion (K,* arrow), *and glial inclusions (C, F, I, L) in the lumber spinal cord of the ALS cases. Note the absence of nuclear staining. Sections are counterstained with hematoxylin to show nuclei in (A–C, E, F, H, I, K, L). Scale bars = 100μm (A, D, G, J); 25μm (B, E, H, K); 12.5μm (C, F, I, L).*

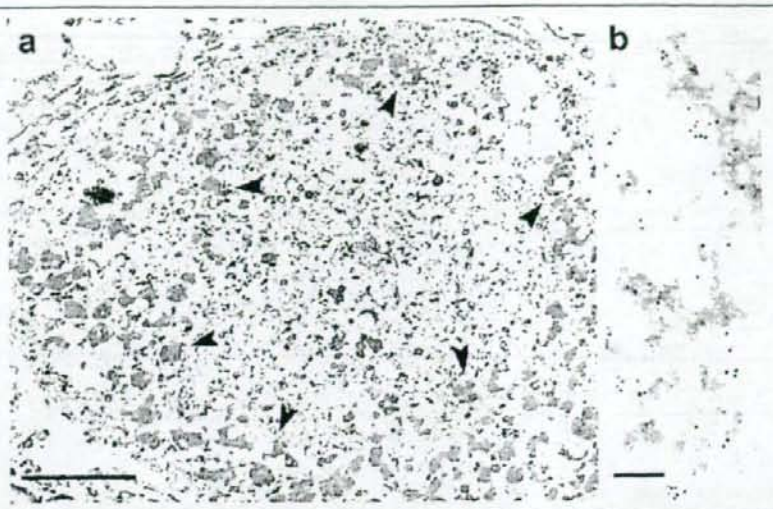

Fig 3. (A) A low-power immunoelectron micrograph of a phosphorylated TAR DNA-binding protein of 43kDa (TDP-43)–positive motoneuronal inclusion in the spinal cord of an amyotrophic lateral sclerosis (ALS) patient. The irregularly shaped structure surrounded by lipofuscins (arrowheads) *is the inclusion. (B) At higher magnification, abnormal filaments of 15nm in diameter are immunopositive. Immunoreaction with pS409/410, probed with immunogold particles (diameter 10nm), appears as* black dots. *Bars = 5μm (A); 500nm (B).*

Phosphorylation Epitopes Are Generated by Casein Kinase-1

To investigate the kinase responsible for the abnormal phosphorylation of TDP-43, we treated recombinant TDP-43 in vitro with CK1, CK2, and GSK3β. Immunoblot analyses of the recombinant TDP-43 showed that phosphorylation by CK1 caused a reduction in gel mobility of TDP-43 to approximately 45kDa and strong immunoreactivity to the phosphorylation-specific antibodies (Fig 6A). TDP-43 phosphorylated by CK2 was only weakly immunoreactive for these antibodies (see Fig 6A), and that phosphorylated by GSK3β was negative (data not shown). Kinase activity capable of generating the approximately 45kDa TDP-43 with pS409/410 epitopes was also detected in crude rat brain extracted with a high concentration (10–20mM) of $MgCl_2$ (data not shown). This kinase activity was not inhibited by the CK2 inhibitor heparin, suggesting that CK1 may be the major kinase in brain extract. Interestingly, increased levels of sodium dodecyl sulfate–stable TDP-43 oligomers were observed after phosphorylation by CK1 (see Fig 6B). Furthermore, based on immunoelectron microscopic analysis, recombinant TDP-43 phosphorylated by CK1 formed abundant filaments when applied on a carbon-coated copper grid (see Fig 6C), whereas nonphosphorylated recombinant TDP-43 formed few filaments (data not shown).

Discussion

We show here that antibodies generated to multiple TDP-43 phosphorylation sites stain the pathological structures in FTLD-U and ALS. These structures include NCIs, NIIs, and DNs in the cerebral cortex and hippocampus, as well as skein-like, round, and glial inclusions in the spinal cord. The phosphorylation-dependent antibodies stain these structures more extensively than an anti-ubiquitin antibody and do not stain normal neuronal nuclei. Furthermore, on immunoelectron microscopy, the phosphorylation-dependent antibodies label abnormal filaments in the motoneuronal inclusion of the ALS case, although these findings may not be the same as for other types of cytoplasmic and intranuclear inclusions.[26] Immunoblot analysis of sarkosyl-insoluble fractions from FTLD-U and ALS brains shows that these antibodies specifically stain abnormal TDP-43 species. These findings are therefore analogous to previous discoveries of phosphorylation-specific epitopes for tau and α-synuclein in tauopathies and α-synucleinopathies.[27–29]

At least five sites on TDP-43 are phosphorylated (Ser 379, Ser 403/404, Ser 409/410) in subjects with FTLD-U and ALS. These results suggest that abnormal phosphorylation takes place mainly near the carboxyl (C)-terminal region of TDP-43. This again is similar to tauopathies and synucleinopathies,[27,28] where multiple Ser residues in the C-terminal region, including

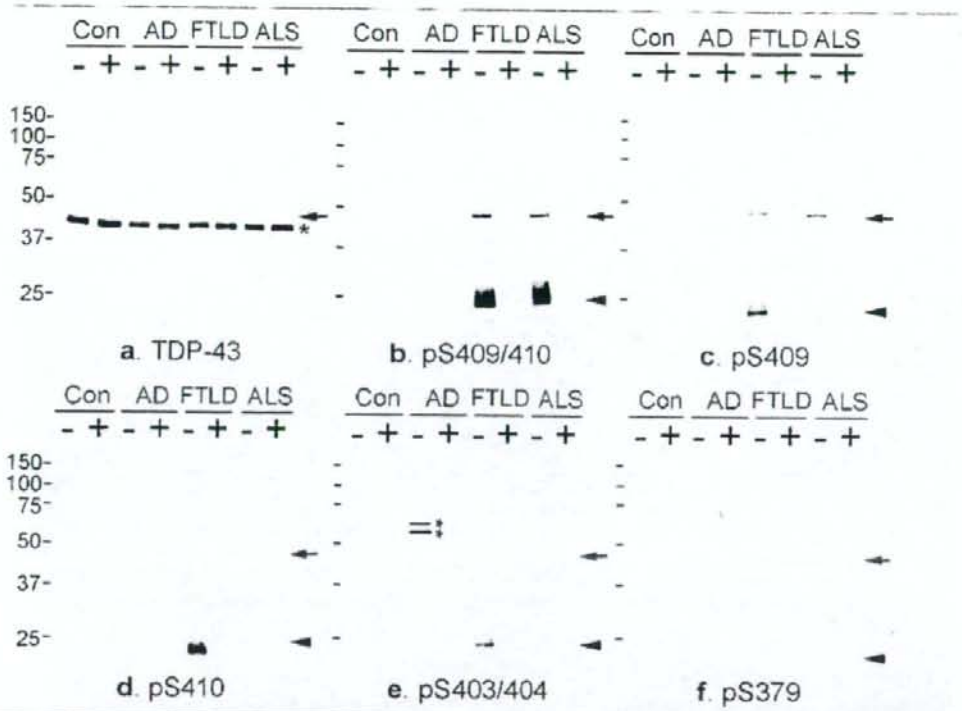

Fig 4. (A) Immunoblot analyses of sarkosyl-insoluble, urea-soluble fractions from control, Alzheimer's disease (AD), frontotemporal lobar degeneration (FTD; frontotemporal lobar degeneration with ubiquitinated inclusions [FTLD-U]), and amyotrophic lateral sclerosis (ALS) brains with phosphorylation-independent anti–TAR DNA-binding protein of 43kDa (TDP-43) antibody (Protein-Tech) (A) and phosphorylation-dependent anti–TDP-43 antibodies specific for pS409/410 (B), pS409 (C), pS410 (D), pS403/404 (E), and pS379 (F) before (−) and after (+) the treatment with lambda protein phosphatase (λPPase). (A) With the phosphorylation-independent antibody, a positive band of 43kDa is commonly seen (asterisk), *whereas an additional band of 45kDa is observed only in FTD and ALS* (arrow), *the labeling of which is abolished after dephosphorylation. (B–F) The phosphorylation-dependent antibodies specifically label the approximately 45kDa band* (arrow) *and the approximately 25kDa fragment* (arrowhead), *as well as a smear, only in FTD and ALS. These immunoreactivities are abolished after dephosphorylation. Normal 43kDa TDP-43 in control and diseased brains is not stained by these phosphorylation-dependent antibodies. The two bands recognized by the antibody specific for pS403/404 in AD (E,* double asterisk*) disappear after dephosphorylation, suggesting a cross-reaction of the antibody to other phosphorylated proteins.*

Ser422 in tau and C-terminal Ser129 in α-synuclein, are abnormally phosphorylated. It has been established that hyperphosphorylated tau and α-synuclein represent the earliest detectable molecular change in the brain in these neurodegenerative diseases.[29,30] Thus, the results of this study suggest that abnormally phosphorylated TDP-43 is a critical component of UPIs in FTLD-U and ALS.

There is a close relation between the pathological subtypes of TDP-43 proteinopathy and the immunoblot pattern of C-terminal fragments of phosphorylated TDP-43. These findings confirm and extend Sampathu and colleagues'[31] and Neumann and coworkers'[12] previous reports that showed C-terminal fragment composition varied between cases with type 1 and 2 pathology. Furthermore, we have shown that cases with type 3 pathology have a band pattern that is mixed or intermediate. These results parallel our earlier findings of differing C-terminal tau fragments in progressive supranuclear palsy and corticobasal degeneration, despite identical composition of tau isoforms.[32] Taken together, these results suggest that elucidating the mechanism of C-terminal fragment origination may shed light on the pathogenesis of several neurodegenerative disorders involving TDP-43 proteinopathy and tauopathy.

These phosphorylation-specific antibodies are a new and powerful tool for the investigation of TDP-43 pro-

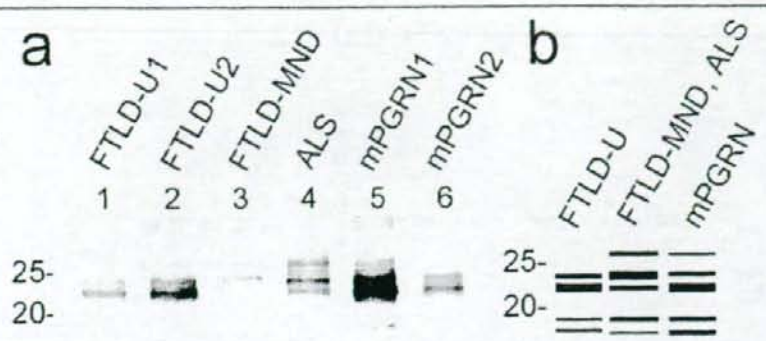

Fig 5. A relation between the clinicopathological subtypes of TAR DNA-binding protein of 43kDa (TDP-43) proteinopathies and the band pattern of the C-terminal fragments of phosphorylated TDP-43. (A) Immunoblots of the sarkosyl-insoluble, urea-soluble fractions from sporadic frontotemporal lobar degeneration with ubiquitinated inclusions (FTLD-U), FTLD-motor neuron disease (MND), amyotrophic lateral sclerosis (ALS), and progranulin mutations (mPGRN) cases with the pS409/410 antibody. The samples are loaded on 15% polyacrylamide gel. Sporadic FTLD-U cases (lanes 1, 2) show a band pattern with 2 major bands at 23 and 24kDa, and 2 minor bands at 18 and 19kDa. A band of 24kDa is weaker than that of 23kDa, and a 19kDa band is weaker than an 18kDa band. FTLD-MND (lane 3) and ALS (lane 4) cases show a pattern with 3 major bands at 23, 24, and 26kDa, and 2 minor bands at 18 and 19kDa. A 24kDa band is the most intense, and an 18kDa band is weaker than a 19kDa band. mPGRN (lanes 5, 6) cases show 3 major bands at 23, 24, and 26kDa, and 2 minor bands at 18 and 19kDa. A 23kDa band is the most intense, and a band of 18kDa and that of 19kDa show similar intensity. The band pattern of mPGRN cases is therefore a composite of that seen in FTLD-U, FTLD-MND, and ALS. (B) Schematic diagram of the band pattern of the C-terminal fragments of phosphorylated TDP-43.

teinopathies. Because phosphorylation-dependent antibodies to TDP-43 react only with abnormally deposited TDP-43, they offer advantages over existing commercially available antibodies for the pathological diagnosis and subtyping of TDP-43 proteinopathies. In addition, and again in analogy with tauopathies, these antibodies may be useful for detecting abnormal TDP-43 in biological fluids such as cerebrospinal fluid.[33]

The results suggest that CK1 is involved in the abnormal phosphorylation and accumulation of TDP-43. In this study, the treatment of recombinant TDP-43 by CK1 generates the same phosphorylation epitopes that are recognized by phosphorylation-dependent antibodies. In addition, phosphorylation at these epitopes facilitates filament formation. In comparison, several protein kinases have been reported to be responsible for phosphorylating tau and α-synuclein. They include, for tau phosphorylation,[34–37] GSK3β, cyclin-dependent kinase 5, mitogen-activated protein kinase, and mitogen-activated protein/microtubule affinity-regulating kinase, and for α-synuclein phosphorylation,[38–40] CK1, CK2, and G-protein–coupled receptor kinase 5.

The pathological significance of phosphorylation of TDP-43 is not clear. It is well known that protein phosphorylation plays an important role in regulating transcription and premessenger RNA splicing. Several splicing factors including hnRNPs, small nuclear ribonucleoproteins, and serine/arginine-rich protein family are known to be phosphorylated in vivo. Various kinases including CK1 have been implicated in phosphorylating these factors.[41–43] Phosphorylation of these factors modulates protein-protein and protein-RNA interactions, and affects their subcellular localization and physiological functions.[31] For instance, Habelhah and colleagues[44] showed that phosphorylation of hnRNP-K by extracellular-signal–regulated kinase results in its cytoplasmic accumulation and also inhibits messenger RNA translation. van der Houven van Oordt and coauthors reported that stress-induced activation of the mitogen-activated protein kinase kinase$_{3/6}$-p38 pathway causes hyperphosphorylation and cytoplasmic accumulation of hnRNP A1, affecting alternative splicing regulation.[45] Thus, phosphorylation of TDP-43 may lead to its cytoplasmic accumulation and influence various physiological functions. Currently, however, it is unclear whether TDP-43 is physiologically phosphorylated in brain. Although in HeLa cells, Ser91 and Ser92 of TDP-43 were reported to be phosphorylated,[46] the antibody specific to pS91/pS92 we made in this study did not stain any structures in normal brains (data not shown). Despite the normal nuclear location of TDP-43, none of the our five phosphorylation-

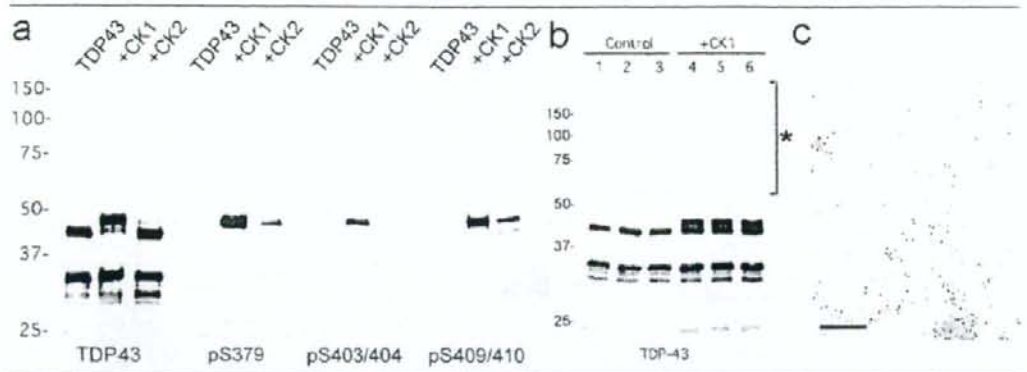

Fig 6. (A) Immunoblot analyses of recombinant TAR DNA-binding protein of 43kDa (TDP-43) phosphorylated in vitro. The crude extract from E. coli *that expressed human TDP-43 is treated with casein kinase-1 (CK1) and CK2 at 30°C for 14 hours, and probed with a phosphorylation-independent antibody against a C-terminal peptide of TDP-43 (405–414), and with phosphorylation-dependent antibodies pS379, pS403/404, and pS409/410. Phosphorylation by CK1 causes the mobility shift to approximately 45kDa and induction of intense immunoreactivity to the phosphorylation-dependent antibodies. (B) Immunoblot analyses of recombinant TDP-43 phosphorylated by CK1. The recombinant TDP-43, which is partially purified by heparin-Toyopearl column chromatography, is incubated with (lanes 4–6) or without (lanes 1–3) CK1 in the presence of adenosine triphosphate at 37°C for 14 hours, and probed with the phosphorylation-independent TDP-43 antibody (ProteinTech). Results in three independent, representative experiments are shown. Note the sodium dodecyl sulfate (SDS)–stable TDP-43 oligomers at approximately 100 to 200kDa* (asterisk) *are detected after phosphorylation by CK1. (C) Positive immunolabeling by pS409/410 of filaments assembled from recombinant TDP-43 phosphorylated by CK1 (10nm colloidal gold). Scale bar = 200nm.*

dependent antibodies stained normal nuclei, suggesting that phosphorylation of these sites is a disease-specific phenomenon.

Our in vitro studies suggest that phosphorylation of TDP-43 facilitates the formation of sodium dodecyl sulfate–stable oligomers and filaments of TDP-43. These abnormal structures may be neurotoxic, as suggested previously for tauopathies and α-synucleinopathies.[30] Thus, abnormal phosphorylation of TDP-43 may be pathological through either a loss of function or a toxic gain of function, or both, leading to the characteristic neuronal degeneration and clinical syndromes.

This research was supported by the Ministry of Education, Culture, Sports, Science and Technology of Japan (Grant-in-Aid for Scientific Research on Priority Areas–Research on Pathomechanisms of Brain Disorders, M.H. (20023038); a Grant-in-Aid for Scientific Research, M.H. (18300117); Grants-in-Aid for Scientific Research, T.A. (19591024), T.N. (19590299)); Grants-in-Aid from the Research Committee of CNS Degenerative Diseases, the Ministry of Health, Labour and Welfare of Japan, I.N. and M.Y. (20261501); the Brain Donation Program at Sun Health Research Institute is supported by the NIH (National Institute on Aging, P30 AG19610), Arizona Alzheimer's Disease Core Center, the Arizona Department of Health Services (contract 211002, Arizona Alzheimer's Research Center), the Arizona Biomedical Research Commission (contracts 4001, 0011, and 05-901), and the Prescott Family Initiative of the Michael J. Fox Foundation for Parkinson's Research; F.B. and E.B. were supported by Telethon Onlus Foundation, Italy (GGP06147) and by a European Community Grant (EURASNET-LSHG-CT-2005-518238).

We thank H. Kondo and Y. Izumiyama for their excellent technical assistance.

References

1. Mackenzie IRA, Feldman HH. Ubiquitin immunohistochemistry suggests classic motor neuron disease, motor neuron disease with dementia, and frontotemporal dementia of the motor neuron disease type represent a clinicopathological spectrum. J Neuropathol Exp Neurol 2005;64:730–739.
2. Baker M, Mackenzie IR, Pickering-Brown SM, et al. Mutations in progranulin cause tau-negative frontotemporal dementia linked to chromosome 17. Nature 2006;442:916–919.
3. Cruts M, Gijselinck I, van der Zee J, et al. Null mutations in progranulin cause ubiquitin-positive frontotemporal dementia linked to chromosome 17q21. Nature 2006;442: 920–924.
4. Watts GDJ, Wymer J, Kovach MJ, et al. Inclusion body myopathy associated with Paget disease of bone and frontotemporal dementia is caused by mutant valosin-containing protein. Nat Genet 2004;36:377–381.
5. Morita M, Al-Chalabi A, Anderson PM, et al. A locus on chromosome 9p confers susceptibility to ALS and frontotemporal dementia. Neurology 2006;66:839–844.
6. Vance C, Al-Chalabi A, Ruddy D, et al. Familial amyotrophic lateral sclerosis with frontotemporal dementia is linked to a locus on chromosome 9p13.2-21.3. Brain 2006;129:868–875.
7. Leigh PN, Anderton BH, Dodson A, et al. Ubiquitin deposits in anterior horn cells in motor neurone disease. Neurosci Lett 1988;93:197–203.
8. Lowe J, Lennox G, Jefferson D, et al. A filamentous inclusion body within anterior horn neurones in motor neurone disease defined by immunocytochemical localization of ubiquitin. Neurosci Lett 1988;94:203–210.

9. Piao YS, Wakabayashi K, Kakita A, et al. Neuropathology with clinical correlations of sporadic amyotrophic lateral sclerosis: 102 autopsy cases examined between 1962 and 2000. Brain Pathol 2003;13:10–22.
10. Ou SH, Wu F, Harrich D, et al. Cloning and characterization of a novel cellular protein, TDP-43, that binds to human immunodeficiency virus type 1 TAR DNA sequence motifs. J Virol 1995;69:3584–3596.
11. Buratti E, Dork T, Zuccato E, et al. Nuclear factor TDP-43 and SR proteins promote in vitro and in vivo CFTR exon 9 skipping. EMBO J 2001;20:1774–1784.
12. Neumann M, Sampathu DM, Kwong LK, et al. Ubiquitinated TDP-43 in frontotemporal lobar degeneration and amyotrophic lateral sclerosis. Science 2006;314:130–133.
13. Arai T, Hasegawa M, Akiyama H, et al. TDP-43 is a component of ubiquitin-positive tau-negative inclusions in frontotemporal lobar degeneration and amyotrophic lateral sclerosis. Biochem Biophys Res Commun 2006;351:602–611.
14. Davidson Y, Kelley T, Mackenzie IRA, et al. Ubiquitinated pathological lesions in frontotemporal lobar degeneration contain the TAR DNA-binding protein, TDP-43. Acta Neuropathol (Berl) 2007;113:521–533.
15. Wang H-Y, Wang I-F, Bose J, Shen C-KJ. Structural diversity and functional implications of the eukaryotic TDP gene family. Genomics 2004;130–139.
16. Buratti E, Brindisi A, Giombi M, et al. TDP-43 binds heterogeneous nuclear ribonucleoprotein A/B through its C-terminal tail. J Biol Chem 2005;280:37572–37584.
17. McKhann GM, Albert MS, Grossman M, et al. Clinical and pathological diagnosis of frontotemporal dementia: report of the work group on frontotemporal dementia and Pick's disease. Arch Neurol 2001;58:1803–1809.
18. Dickson DW, Josephs KA, Amador-Ortiz C. TDP-43 in differential diagnosis of motor neuron disorders. Acta Neuropathol (Berl) 2007;114:71–79.
19. Newell KL, Hyman BT, Growdon JH, Hedley-Whyte ET. Application of the National Institute on Aging (NIA)-Reagan Institute criteria for the neuropathological diagnosis of Alzheimer disease. J Neuropathol Exp Neurol 1999;58:1147–1155.
20. Kitagawa T, Aikawa T. Enzyme coupled immunoassay of insulin using a novel coupling reagent. J Biochem (Tokyo) 1976; 79:233–236.
21. Mori H, Kondo J, Ihara Y. Ubiquitin is a component of paired helical filaments in Alzheimer's disease. Science 1987;235: 1641–1644.
22. Arima K, Mizutani T, Alim MA, et al. NACP/alpha-synuclein and tau constitute two distinctive subsets of filaments in the same neuronal inclusions in brains from a family of parkinsonism and dementia with Lewy bodies: double-immunolabeling fluorescence and electron microscopic studies. Acta Neuropathol (Berl) 2000;100:115–121.
23. Hasegawa M, Arai T, Akiyama H, et al. TDP-43 is deposited in the Guam parkinsonism-dementia complex brains. Brain 2007;130:1386–1394.
24. Cairns NJ, Bigio EH, Mackenzie IR, et al. Neuropathologic diagnostic and nosologic criteria for frontotemporal lobar degeneration: consensus of the Consortium for Frontotemporal Lobar Degeneration. Acta Neuropathol (Berl) 2007;114:5–22.
25. Snowden J, Neary D, Mann D. Frontotemporal lobar degeneration: clinical and pathological relationships. Acta Neuropathol (Berl) 2007;114:31–38.
26. Amador-Ortiz C, Lin WL, Ahmed Z, et al. TDP-43 immunoreactivity in hippocampal sclerosis and Alzheimer's disease. Ann Neurol 2007;61:435–445.
27. Hasegawa M, Jakes R, Crowther RA, et al. Characterization of mAb AP422, a novel phosphorylation-dependent monoclonal antibody against tau protein. FEBS Lett 1996;384:25–30.
28. Fujiwara H, Hasegawa M, Dohmae N, et al. α-Synuclein is phosphorylated in synucleinopathy lesions. Nat Cell Biol 2002; 4:160–164.
29. Goedert M, Spillantini MG, Davies SW. Filamentous nerve cell inclusions in neurodegenerative diseases. Curr Opin Neurobiol 1998;8:619–632.
30. Goedert M. The significance of tau and alpha-synuclein inclusions in neurodegenerative diseases. Curr Opin Genet Dev 2001;11:343–351.
31. Sampathu DM, Neumann M, Kwong LK, et al. Pathological heterogeneity of frontotemporal lobar degeneration with ubiquitin-positive inclusions delineated by ubiquitin immunohistochemistry and novel monoclonal antibodies. Am J Pathol 2006;169:1343–1352.
32. Arai T, Ikeda K, Akiyama H, et al. Identification of amino-terminally cleaved tau fragments that distinguish progressive supranuclear palsy from corticobasal degeneration. Ann Neurol 2004;55:72–79.
33. Ishiguro K, Ohno H, Arai H, et al. Phosphorylated tau in human cerebrospinal fluid is a diagnostic marker for Alzheimer's disease. Neurosci Lett 1999;270:91–94.
34. Ishiguro K, Takamatsu M, Tomizawa K, et al. Tau protein kinase I converts normal tau protein into A68-like component of paired helical filaments. J Biol Chem 1992;267:10897–10901.
35. Baumann K, Mandelkow EM, Biernat J, et al. Abnormal Alzheimer-like phosphorylation of tau-protein by cyclin-dependent kinases cdk2 and cdk5. FEBS Lett 1993;336: 417–424.
36. Drewes G, Lichtenberg-Kraag B, Döring F, et al. Mitogen activated protein (MAP) kinase transforms tau protein into an Alzheimer-like state. EMBO J 1992;11:2131–2138.
37. Drewes G, Ebneth A, Preuss U, et al. MARK, a novel family of protein kinases that phosphorylate microtubule-associated proteins and trigger microtubule disruption. Cell 1997;89: 297–308.
38. Ishii A, Nonaka T, Taniguchi S, et al. Casein kinase 2 is the major enzyme in brain that phosphorylates Ser129 of human alpha-synuclein: implication for alpha-synucleinopathies. FEBS Lett 2007;581:4711–4717.
39. Arawaka S, Wada M, Goto S, et al. The role of G-protein-coupled receptor kinase 5 in pathogenesis of sporadic Parkinson's disease. J Neurosci 2006;26:9227–9238.
40. Pronin AN, Morris AJ, Surguchov A, Benovic JL. Synucleins are a novel class of substrates for G protein-coupled receptor kinases. J Biol Chem 2000;275:26515–26522.
41. Soret J, Tazi J. Phosphorylation-dependent control of the pre-mRNA splicing machinery. Prog Mol Subcell Biol 2003;31: 89–126.
42. Gross SD, Loijens JC, Anderson RA. The casein kinase Ialpha isoform is both physically positioned and functionally competent to regulate multiple events of mRNA metabolism. J Cell Sci 1999;112:2647–2656.
43. Mayrand SH, Dwen P, Pederson T. Serine/threonine phosphorylation regulates binding of C hnRNP proteins to pre-mRNA. Proc Natl Acad Sci USA 1993;90:7764–7768.
44. Habelhah H, Shah K, Huang L, et al. ERK phosphorylation drives cytoplasmic accumulation of hnRNP-K and inhibition of mRNA translation. Nat Cell Biol 2001;3:325–330.
45. van der Houven van Oordt W, Diaz-Meco MT, Lozano J, et al. The MKK(3/6)-p38-signaling cascade alters the subcellular distribution of hnRNP A1 and modulates alternative splicing regulation. J Cell Biol 2000;149:307–316.
46. Olsen JV, Blagoev B, Gnad F, et al. Global, in vivo, and site-specific phosphorylation dynamics in signaling networks. Cell 2006;127:635–648.

Inverse Ocular Bobbing in a Patient With Encephalitis Associated With Antibodies to the *N*-methyl-D-aspartate Receptor

A 30-YEAR-OLD WOMAN presented with headache, fever, disorientation, and recent memory disturbance. Brain magnetic resonance imaging showed fluid-attenuated inversion recovery hyperintense abnormalities in both hippocampi, without abnormal findings in other areas of the brain or brainstem.[1] The patient subsequently developed tonic convulsions, restlessness, anxiety, and hypoventilation that led to the use of sedation and mechanical ventilation. While in the intensive care unit, inverse ocular bobbing and skew deviation were transiently observed (**Figure**) (a video is available at http://www.archneurol.com). Antibodies to NR1/NR2 heteromers of the *N*-methyl-D-aspartate receptor were identified in her serum and cerebrospinal fluid. After immunotherapy and removal of an ovarian teratoma, all symptoms started to improve and the patient was able to return to her job 1 year later.

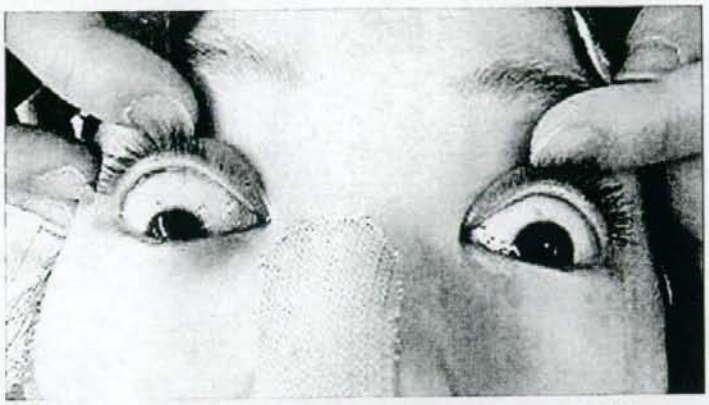

Figure. The position of the patient's eyes showed skew deviation when the inverse ocular bobbing resolved.

COMMENT

Inverse ocular bobbing, or ocular dipping, consists of a slow, spontaneous downward eye movement with fast return to midposition. In contrast to ocular bobbing, which is most often attributed to large, destructive pontine lesions, ocular dipping may be observed in anoxic coma or following prolonged status epilepticus and is thought to be a marker of diffuse, rather than focal, brain damage.[2] The encephalitis associated with antibodies to the *N*-methyl-D-aspartate receptor often associates with central hypoventilation and, much less frequently, with vertical gaze paresis or cranial nerve dysfunction, all suggesting involvement of the brainstem.[3] In the current case with head magnetic resonance images that did not show any signal abnormality in the brainstem, the association of ocular dipping with hypoventilation and skew deviation suggests that the diffuse encephalopathy in addition to involvement of the brainstem ocular pathways were responsible for the abnormal ocular movement.

Video available online at www.archneurol.com

Haruo Shimazaki, MD, PhD
Mitsuya Morita, MD, PhD
Imaharu Nakano, MD, PhD
Josep Dalmau, MD, PhD

Correspondence: Dr Shimazaki, Division of Neurology, Department of Internal Medicine, Jichi Medical University, Yakushiji 3311-1, Shimotsuke, Tochigi 329-0498, Japan (hshimaza@jichi.ac.jp).

Author Contributions: *Study concept and design:* Shimazaki and Nakano. *Acquisition of data:* Shimazaki and Morita. *Analysis and interpretation of data:* Shimazaki, Morita, and Dalmau. *Drafting of the manuscript:* Shimazaki. *Critical revision of the manuscript for important intellectual content:* Shimazaki, Morita, Nakano, and Dalmau. *Administrative, technical, and material support:* Shimazaki. *Study supervision:* Morita, Nakano, and Dalmau.

Financial Disclosure: None reported.

Funding/Support: This work was partially supported by a Grant-in-Aid for Scientific Research (C) (20591009 to Dr Shimazaki) of The Ministry of Education, Culture, Sports, Science and Technology in Japan.

Additional Information: Video is available at http://www.archneurol.com.

REFERENCES

1. Shimazaki H, Ando Y, Nakano I, Dalmau J. Reversible limbic encephalitis with antibodies against the membranes of neurones of the hippocampus. *J Neurol Neurosurg Psychiatry*. 2007;78(3):324-325.
2. Leigh RJ, Zee DS. *The Neurology of Eye Movements*. 4th ed. New York, NY: Oxford University Press; 2006:674-675.
3. Dalmau J, Tuzun E, Wu HY, et al. Paraneoplastic anti-*N*-methyl-D-aspartate receptor encephalitis associated with ovarian teratoma. *Ann Neurol*. 2007; 61(1):25-36.

Acta Neuropathol (2008) 115:561–575
DOI 10.1007/s00401-007-0329-z

ORIGINAL PAPER

Basophilic inclusion body disease and neuronal intermediate filament inclusion disease: a comparative clinicopathological study

Osamu Yokota · Kuniaki Tsuchiya · Seishi Terada · Hideki Ishizu · Hirotake Uchikado · Manabu Ikeda · Kiyomitsu Oyanagi · Imaharu Nakano · Shigeo Murayama · Shigetoshi Kuroda · Haruhiko Akiyama

Received: 19 October 2007 / Revised: 30 November 2007 / Accepted: 1 December 2007 / Published online: 13 December 2007

Abstract While both neuronal intermediate filament inclusion disease (NIFID) and basophilic inclusion body disease (BIBD) show frontotemporal lobar degeneration and/or motor neuron disease, it remains unclear whether, and how, these diseases differ from each other. Here, we compared the clinicopathological characteristics of four BIBD and two NIFID cases. Atypical initial symptoms included weakness, dysarthria, and memory impairment in BIBD, and dysarthria in NIFID. Dementia developed more than 1 year after the onset in some BIBD and NIFID cases. Upper and lower motor neuron signs, parkinsonism, and parietal symptoms were noted in both diseases, and involuntary movements in BIBD. Pathologically, severe caudate atrophy was consistently found in both diseases. Cerebral atrophy was distributed in the convexity of the fronto-parietal region in NIFID cases. In both BIBD and NIFID, the frontotemporal cortex including the precentral gyrus, caudate nucleus, putamen, globus pallidus, thalamus, amygdala, hippocampus including the dentate gyrus, substantia nigra, and pyramidal tract were severely affected, whereas lower motor neuron degeneration was minimal. While α-internexin-positive inclusions without cores were found in both NIFID cases, one NIFID case also had α-internexin- and neurofilament-negative, but p62-positive, cytoplasmic spherical inclusions with eosinophilic p62-negative cores. These two types of inclusions frequently coexisted in the same neuron. In three BIBD cases, inclusions were tau-, α-synuclein-, α-internexin-, and neurofilament-negative, but

O. Yokota · K. Tsuchiya · H. Akiyama
Department of Neuropathology,
Tokyo Institute of Psychiatry,
2-1-8 Kamikitazawa, Setagaya-ku,
Tokyo 156-8585, Japan

O. Yokota (✉) · S. Terada · H. Ishizu · S. Kuroda
Department of Neuropsychiatry,
Okayama University Graduate School of Medicine,
Dentistry and Pharmaceutical Sciences,
2-5-1 Shikata-cho, Okayama 700-8558, Japan
e-mail: oyokota1@yahoo.co.jp

K. Tsuchiya
Department of Laboratory Medicine and Pathology,
Tokyo Metropolitan Matsuzawa Hospital, Tokyo, Japan

K. Tsuchiya
Department of Neurology,
Tokyo Metropolitan Matsuzawa Hospital, Tokyo, Japan

H. Ishizu
Department of Laboratory Medicine,
Zikei Institute of Psychiatry, Okayama, Japan

H. Uchikado
Department of Psychiatry,
Yokohama City University School of Medicine,
Yokohama, Japan

M. Ikeda
Department of Psychiatry and Neuropathobiology,
Kumamoto University Graduate School of Medical Sciences,
Kumamoto, Japan

K. Oyanagi
Department of Neuropathology,
Tokyo Metropolitan Institute for Neuroscience, Tokyo, Japan

I. Nakano
Division of Neurology, Department of Medicine,
Jichi Medical University School of Medicine, Tochigi, Japan

S. Murayama
Department of Neuropathology,
Tokyo Metropolitan Institute of Gerontology, Tokyo, Japan

occasionally p62-positive. These findings suggest that: (1) the clinical features and distribution of neuronal loss are similar in BIBD and NIFID, and (2) an unknown protein besides α-internexin and neurofilament may play a pivotal pathogenetic role in at least some NIFID cases.

Keywords α-Internexin · Caudate nucleus · Frontotemporal dementia · TDP-43 · Motor neuron disease

Introduction

Basophilic inclusion body disease (BIBD) is a rare disease entity, whose clinical phenotype includes dementia and motor neuron disease (MND) [25]. Cases of dementia having basophilic inclusions were originally called "generalized variant of Pick's disease" [24]. The clinical and pathological features of BIBD were reported to be young onset, remarkable degeneration in the frontotemporal cortex, caudate nucleus, and substantia nigra, and the occurrence of round cytoplasmic basophilic inclusions immunonegative for tau or neurofilament. As far as we know, only seven autopsy cases of generalized variant of Pick's disease have been reported [11, 14, 24, 36]. Like the generalized variant of Pick's disease, the onset age in MND cases with basophilic inclusions reported previously is very young, often under 40 years. MND with basophilic inclusions is also very rare, and only about ten cases of this subtype have been reported [1, 13, 18, 19, 22, 23, 28, 30, 33, 34, 37, 41].

Recently, a new disease entity of frontotemporal lobar degeneration (FTLD) called neuronal intermediate filament inclusion disease (NIFID), neurofilament inclusion body disease (NIBD), or neurofilament inclusion disease (NFID) was proposed [5, 6, 16]. A pathological hallmark of NIFID is the occurrence of neurofilament-positive intraneuronal inclusions. More recently, it was reported that α-internexin immunohistochemistry reveals the inclusions more sensitively and specifically [6, 39].

The morphological features of the inclusions in NIFID on conventional stains are quite similar to those of inclusions in BIBD. Further, the BIBD cases previously reported were not always fully examined immunohistochemically. Therefore, the clinical and pathological characteristics in BIBD have not been fully established, and whether the clinicopathological features of BIBD are different from those of NIFID remains unclear. In the present study, we first used α-internexin and neurofilament immunohistochemistry to differentiate NIFID cases from our series of cases that were previously diagnosed as BIBD, based on conventional stains. Then, we compared the clinical features, distribution of neuronal loss, and immunohistochemical characteristics of BIBD and NIFID cases.

Materials and methods

Subjects

Six cases previously diagnosed as BIBD were selected from our autopsy series. A diagnosis of BIBD had been made based on the conventional histopathological features of basophilic inclusion bodies reported previously: (1) round or oval intraneuronal inclusions that are detected by hematoxylin-eosin (H&E), Klüver-Barrera, and Bodian stains according to previous reports [24] and (2) that are not immunolabeled with antibodies against tau, α-synuclein, or ubiquitin. The six cases were immunohistochemically reexamined.

Neuropathological examination

Brain tissue samples from all subjects were fixed postmortem with 10% formalin and embedded in paraffin. Sections (10 μm thick) from the frontal, temporal, parietal, occipital, insular, and cingulate cortices, hippocampus, amygdala, basal ganglia, midbrain, pons, medulla oblongata, cerebellum, and spinal cord were prepared. These sections were stained by the hematoxylin-eosin (H&E), Klüver-Barrera, Holzer, methenamine silver, Bodian, and Gallyas-Braak methods.

Sections from representative regions of the cerebrum, brainstem, and spinal cord were examined immunohistochemically using antibodies to ubiquitin (Z0458, rabbit, polyclonal, 1:5,000, Dako, Glostrup, Denmark), ubiquitin (MAB1510, mouse, monoclonal, 1:500, Chemicon, Burlingame, CA, USA), phosphorylated tau (AT8, mouse, monoclonal, 1:3,000, Innogenetics, Ghent, Belgium), phosphorylated neurofilament (SMI31, mouse, monoclonal, 1:1,000, Sternberger, Lutherville, MD, USA), phosphorylation-independent neurofilament (SMI32: mouse, monoclonal, 1:100, Sternberger Monoclonals, Baltimore, MD, USA), α-internexin (ab32306, rabbit, polyclonal, 1:100, Abcam Plc., Cambridge, UK), phosphorylated α-synuclein (psyn#64, mouse, monoclonal, 1:1,000, Wako, Osaka, Japan), TDP-43 (10782-1-AP, rabbit, polyclonal, 1:500, ProteinTech Group Inc., Chicago, IL, USA), N-terminus of p62 protein (p62-N, guinea pig, polyclonal, 1:500, Progen Biotechnik GmbH, Heidelberg, Germany), C-terminus of p62 protein (p62-C, guinea pig, polyclonal, 1:500, Progen Biotechnik GmbH), polyglutamine (1C2, mouse, monoclonal, 1:10,000, Chemicon, Burlingame, CA, USA), and glial fibrillary acidic protein (GFAP, rabbit, polyclonal, 1:5,000, Dako). Deparaffinized sections were incubated with 1% H_2O_2 in methanol for 20 min to eliminate endogenous peroxidase activity in the tissue. Sections were treated with 0.2% TritonX-100 for 5 min and washed in phosphate-buffered saline (PBS, pH 7.4). When using anti-ubiquitin, anti-neurofilament,

anti-N-terminus p62, anti-C-terminus p62, and anti-α-internexin antibodies, the sections were pretreated by autoclaving for 10 min in 10 mM sodium citrate buffer at 120°C. After blocking with 10% normal serum, the sections were incubated for 72 h at 4°C with one of the primary antibodies in 0.05 M *Tris*–HCl buffer, pH 7.2, containing 0.1% Tween and 15 mM NaN_3. After three 10-min washes in PBS, the sections were incubated in biotinylated anti-rabbit, anti-mouse, or anti-guinea pig secondary antibody for 1 h, and then in avidin-biotinylated horseradish peroxidase complex (ABC Elite kit, Vector, Burlingame, CA, USA) for 1 h. The peroxidase labeling was visualized with 0.2% 3,3′-diaminobenzidine (DAB) as the chromogen. The sections were counterstained with hematoxylin. For double staining with N-terminal-specific p62 antibody (p62-N) and anti-α-internexin antibody (ab32306), primary antibody labeling in the first cycle (p62-N) was detected in the same way as single staining except that the DAB reaction was intensified with nickel ammonium sulfate to yield a dark purple precipitate. Then, primary antibody labeling in the second cycle (ab32306) was detected in the same way as single staining. The sections were counterstained with nuclear fast red for double immunostaining.

Semiquantitative assessment of histopathological lesions

Neuronal loss and gliosis in representative regions were semiquantitatively evaluated. The degree of degeneration in the cerebral cortex was assessed on H&E-, KB-, and GFAP-stained sections according to the following grading system employed in our previous study [43]: −, no histopathological alteration; +, slight neuronal loss and gliosis are observed only in the superficial layers; ++, obvious neuronal loss and gliosis are found in cortical layers II and III, and status spongiosis and relative preservation of neurons in layers V and VI are often present; and +++, pronounced neuronal loss with gliosis is found in all cortical layers, and the adjacent subcortical white matter exhibits prominent fibrous gliosis. In the basal ganglia and brainstem nuclei, the degree of neuronal loss and gliosis was assessed on H&E-, KB-, and GFAP-stained sections according to the following grading system: -, neither neuronal loss nor gliosis is observed; ±, mild gliosis is observed on H&E- or GFAP-immunostained sections, but neurons are not reduced in number; +, mild gliosis and mild neuronal loss are present; ++, neuronal loss and gliosis are moderate, but tissue rarefaction is absent; and +++, severe neuronal loss, severe fibrous gliosis, and tissue rarefaction are observed. Degeneration of the corticospinal tract at the level of the cerebral peduncle and medulla oblongata and of the frontopontine tract in the cerebral peduncle was assessed by loss of myelin, glial proliferation, and presence of macrophages, and indicated as + (present) or − (absent).

Results

Among six cases previously diagnosed as BIBD, neurofilament-positive inclusions were disclosed in two cases, and the inclusions also showed intense immunoreactivity to α-internexin; thus, the diagnosis of these cases was changed to NIFID. The other four cases were again diagnosed as BIBD. Limited clinical and pathological data in cases 1 [9], 2 [15], 3 [20], 5 [32, 36], and 6 [42] have been reported in Japanese.

Case reports

Case 1 (BIBD)

This man was 40 years old at the time of death. He initially complained of difficulty working in high places at age 34. Subsequently, weakness in the left hand and dysarthria developed. Neurological examination at age 35 revealed muscle weakness, fasciculation, and cerebellar ataxia including lack of coordination of the left side extremities. Apathy and oral dyskinesia also developed. Subsequently, involuntary movements such as an alien-hand sign to grasp something with the left hand, deviation of the tongue to the right side, and spastic paralysis in the left extremities also emerged. He obtained an IQ score of 89 on the Wechsler Adult Intelligence Scale (WAIS). At age 36, he could not walk without support. Reduction of utterance, impaired comprehension of speech, disorientation, bradykinesia, swallowing disturbance, ideomotor apraxia, and dressing apraxia were found. Weakness of the left facial muscles and four extremities, muscle atrophy of the tongue, left sternocleidomastoid muscle, and hands, and fasciculation of the legs were also observed. Deep tendon reflexes were hyperactive, and the Babinski sign was positive on the right side. Examinations of blood and cerebrospinal fluid were unremarkable. Electromyography and nerve conduction velocity testing were within normal limits, and neurogenic patterns were observed on muscle biopsy specimens. He died of pneumonia, with a clinical course of 6 years and 4 months. The final neurological diagnosis was amyotrophic lateral sclerosis (ALS) with dementia or Creutzfeldt-Jakob disease.

Case 2 (BIBD)

The patient was a man who was 63 years old at the time of death. He initially developed obsessive ideas and behaviors at the age of 57 years. Subsequently, stereotypic behaviors occurred. He had no relevant past medical or family history. Neurological examination at age 57 disclosed obsessive behaviors, impaired facial recognition, euphoria, and emotional incontinence. Baseline blood examinations were

within normal limits. He was tested using the WAIS and obtained an IQ score of 99. At age 58, apathy, restlessness, oral tendency, disorientation in time and place, impaired memory function, and disturbance of calculation ability were observed. No motor neuron signs, parkinsonism, or cerebellar symptoms were noted, and his gait was normal. He obtained an IQ score of 77 on the WAIS. Parkinsonism first developed at age 59 and primitive reflexes at age 63. He died about 6 years after the onset. The final neurological diagnosis was Pick's disease.

Case 3 (BIBD)

This was a housewife who was 67 years at the time of death. She presented initially with an obsession with collecting things at the age of 56. Subsequently, memory disturbance occurred. She neglected her housework and began to eat only rice and pickled vegetables. At age 58, she was inflexible, drinking too much, and had pica. She had no relevant past medical or family history. Neurological examination at age 58 revealed memory disturbance, impairment of calculation ability, disorientation, emotional unconcern, verbal perseveration, and lack of insight. Blood, urine, and cerebrospinal fluid examinations were within normal limits. Thereafter, double incontinence, verbal stereotypy, echolalia, and reduction of spontaneous speech output were found. She became bedridden at age 60. At age 65, involuntary movements like chorea of the head, four extremities, and trunk occurred. This was a quick, small movement, and she shook her head to the right or left side. In addition, athetosis-like movements of the left arm developed. She died of cardiac failure with a clinical course of 12 years. Her neurological diagnosis was Pick's disease.

Case 4 (BIBD)

This was a 47-year-old man at the time of death. His initial symptom was self-centered behavior at the age of 40; subsequently, disinhibition, irritability, and stereotypic behaviors also occurred. He had no relevant past medical or family history. Neurological examination at age 42 disclosed indifference and lack of insight. The snout reflex was positive. Memory disturbance, aphasia, and constructional impairment were not found. A verbal fluency test revealed poor generation of words (animals = 10, letters = 4). He scored 27/30 on the MMSE (cut off: 24/25) and 25/36 on Raven's Colored Progressive Matrices (cut-off: 24/25). On the WAIS-Revised (WAIS-R), he obtained a verbal IQ score of 77, performance IQ score of 68, and full-scale IQ score of 70. On the Wechsler Memory Scale-Revised (WMS-R, mean ± standard deviation in all subscales = 100 ± 15), he obtained scores on verbal memory of 64, visual memory of 57, general memory of 50, attention/concentration of 80, and delayed recall <50. Restlessness, irritability, and social breakdown became increasingly remarkable. Thereafter, bilateral forced grasping, rigidity in the four extremities, retrocollis, reduction of utterance, aspontaneity, and sexual disinhibition developed. He died of pneumonia with a clinical course of about 7 years. His neurological diagnosis was the frontal-predominant type of Pick's disease.

Case 5 (NIFID)

This was a 73-year-old woman at the time of death. She presented initially with difficulty speaking clearly at the age of 67 years. Thereafter, she was aware of writing incomprehensible sentences. She had no relevant past medical or family history. Neurological examination at age 68 disclosed dysarthria, forced laughing, and effortful and monotonous speech output. Palatal reflex and pharyngeal reflex were decreased. Muscle weakness, atrophy, fasciculation, or pathological reflex was not found. Deep tendon reflex was slightly increased in the four extremities. Upward gaze was slightly restricted. Buccofacial apraxia was found. Baseline blood, urine, and cerebrospinal fluid examinations were unremarkable. An electromyogram was within normal limits. Verbal IQ and performance IQ scores tested by the WAIS-R were 100 and 87, respectively, and a full-scale IQ score was 94. She scored 161/165 on the Token test. She showed poor results on the Wisconsin Card Sorting test, presumably because of an inability to shift attention and frontal dysfunction, attaining only one category with frequent perseverative errors. On the Western Aphasia Battery (WAB), she scored 8/10 for information content, 9.2/10 for auditory word recognition, 4.2/10 for repetition, 8.6/10 for object naming, 6/10 for word fluency, 9.8/10 for reading aloud, and 10/10 for spontaneous writing. Abilities of naming, aural comprehension, and reading were preserved. On the WMS-R, she scored 128 for verbal memory, 68 for visual memory, 84 for general memory, 80 for attention/concentration, and 74 for delayed memory. At age 69, swallowing disturbance, repetitive motor actions, and gait instability occurred, and her utterance was limited to moans. Thereafter, vertical supranuclear gaze palsy, bradykinesia, rigidity, anterocollis, forced grasping, bilateral Babinski signs, dressing apraxia, fasciculation of the tongue, and myoclonus in the left arm developed. She died of pneumonia with a clinical course of 5 years and 8 months. The neurological diagnosis was slowly progressive aphasia.

Case 6 (NIFID)

A 29-year-old forwarding agent became aware of his disinhibited and self-centered behaviors. He started borrowing